Biological Role and Therapeutic Targeting of TGF- 3 in Glioblastoma

Seystahl, Katharina ; Papachristodoulou, Alexandros ; Burghardt, Isabel ; Schneider, Hannah ; Hasenbach, Kathy ; Janicot, Michel ; Roth, Patrick ; Weller, Michael

DOI: https://doi.org/10.1158/1535-7163.MCT-16-0465

Biological role and therapeutic targeting of TGF-β3 in glioblastoma

Katharina Seystahl[1], Alexandros Papachristodoulou[1], Isabel Burghardt[1], Hannah Schneider[1], Kathy Hasenbach[1,2], Michel Janicot[2], Patrick Roth[1], Michael Weller[1]

[1]Laboratory of Molecular Neuro-Oncology, Department of Neurology, University Hospital and University of Zurich, Switzerland

[2]Isarna Therapeutics GmbH, Munich, Germany

Correspondence to: Katharina Seystahl, Department of Neurology, University Hospital Zurich, Zurich Switzerland, phone +41 255 5500, fax +41 44 255 4380, E-Mail: katharina.seystahl@usz.ch

Running title: Targeting TGF-β3 in glioblastoma

Keywords: Glioblastoma, TGF-β

Financial support:

This study was supported by a research grant from Isarna (Munich, Germany), a grant from the Swiss Cancer League/Oncosuisse to I. Burghardt and M. Weller (project number KFS-3305-08-2013), and by a grant of the Canton of Zurich (HSM-2) to M. Weller and P. Roth.

Abbreviations list

Glioma-initiating cell (GIC)

Long-term malignant glioma cell lines (LTC)

Plasminogen activator inhibitor (PAI)

SD (standard deviation)

Transforming growth factor (TGF)

Abstract

Transforming growth factor (TGF)-β contributes to the malignant phenotype of glioblastoma by promoting invasiveness and angiogenesis and creating an immunosuppressive microenvironment. So far, TGF-β1 and TGF-β2 isoforms have been considered to act in a similar fashion without isoform-specific function in glioblastoma. A pathogenic role for TGF-β3 in glioblastoma has not been defined yet. Here we studied the expression and functional role of endogenous and exogenous TGF-β3 in glioblastoma models. *TGF-β3* mRNA is expressed in human and murine long-term glioma cell lines as well as in human glioma-initiating cell cultures with expression levels lower than *TGF-β1* or *TGF-β2* in most cell lines. Inhibition of *TGF-β3* mRNA expression by ISTH2020 or ISTH2023, two different isoform-specific phosphorothioate locked nucleic acid (LNA)-modified antisense oligonucleotide gapmers, blocks down-stream SMAD2 and SMAD1/5 phosphorylation in human LN-308 cells, without affecting *TGF-β1* or *TGF-β2* mRNA expression or protein levels. Moreover, inhibition of *TGF-β3* expression reduces invasiveness *in vitro*. Interestingly, depletion of *TGF-β3* also attenuates signaling evoked by TGF-β1 or TGF-β2. In orthotopic syngeneic (SMA-560) and xenograft (LN-308) *in vivo* glioma models, expression of *TGF-β3* as well of the down-stream target, *plasminogen-activator-inhibitor (PAI)-1,* was reduced while *TGF-β1* and *TGF-β2* levels were unaffected following systemic treatment with *TGF-β3*-specific antisense oligonucleotides.

We conclude that TGF-β3 might function as a gatekeeper controlling down-stream signaling despite high expression of TGF-β1 and TGF-β2 isoforms. Targeting TGF-β3 *in vivo* may represent a promising strategy interfering with aberrant TGF-β signaling in glioblastoma.

Introduction

Transforming growth factor (TGF)-β is a pleiotropic cytokine with multiple effects on cellular behavior including proliferation, migration, invasion, angiogenesis and immune responsiveness. The three TGF-β isoforms, TGF-β1, TGF-β2 and TGF-β3, exhibit high levels of similarity in their amino acid sequences, however, the tertiary structure of the active domain of TGF-β3 differs from TGF-β1 and TGF-β2, enabling steric rearrangements which allow a more flexible binding to TGF-β receptor II (TβRII) (1-5). TGF-β3 has an isoform-specific function in embryonic palate fusion and wound healing (6-8). The deficits of TGF-β3 knockout mice are almost exclusively restricted to impaired palate fusion and pulmonary abnormalities (9). In contrast, mice with a gene knockout for TGF-β1 or TGF-β2 exhibit multi-organ deficits, TGF-β1 especially in the hematopoietic and vasculogenic system and TGF-β2 in multiple embryonal developmental processes including the development of heart, lung, neurons and bones (10, 11). The different phenotypes of TGF-β isoform knockout mice point towards non-overlapping isotype-specific functions. Reports on TGF-β3 in cancer are almost exclusively restricted to expression analyses and correlative studies without revealing an isotype-specific functional role (5).

Aberrant TGF-β signaling is considered as a hallmark for the malignant phenotype of glioblastoma. All the three TGF-β isoforms, TGF-β1, TGF-β2 and TGF-β3 are expressed in malignant gliomas *in vivo* (12, 13). However, pathogenic effects in glioblastoma have been only attributed to the isoforms TGF-β1 and TGF-β2 while there are no functional data for TGF-β3 (14-16).

Molecular subtyping has identified TGF-β3 as a gene highly expressed in the classical glioblastoma subtype (17). Still, the functional role of TGF-β3 in the malignant phenotype of glioblastoma remains uncertain, and its mRNA expression

levels *in vivo* are lower than those of TGF-β1 and TGF-β2 (13). Here, we characterize the expression and biological activity of TGF-β3 using isoform-specific oligonucleotides in human and murine glioma models.

Materials and methods

Cell culture

Nine human long-term malignant glioma cell lines (LTC), obtained in 1994, were previously described (18) and sent for authentification tests to the German Biological Resource Centre DSMZ in Braunschweig, Germany, in November 2013. The spontaneous murine astrocytoma (SMA) cell lines (SMA-497, SMA-540, and SMA-560) kindly provided by Dr D. Bigner (Durham, NC) were previously characterized (19-21). Murine GL-261 cells were obtained from the National Cancer Institute (Frederick, MD). Five human glioma-initiating cell (GIC) lines, established after informed consent and approval of the local ethics committees have been previously described (22-24).

Reagents

Human and murine LTC were cultured in Dulbecco´s modified Eagle´s medium supplemented with 10% fetal calf serum. GIC were maintained in Neurobasal Medium supplemented with B-27 (20 µl/ml) and glutamine (10 µl/ml) from Invitrogen (Basel, Switzerland), fibroblast growth factor-2 and epidermal growth factor (20 ng/ml each; Peprotech, Rocky Hill, PA). Recombinant TGF-β1, TGF-β2, and TGF-β3 (R&D, Minneapolis, MN) were used as indicated. TGF-β3-targeted oligonucleotides ISTH2020, ISTH2023 and control oligonucleotide C3_ISTH0047 were designed and provided by Isarna Therapeutics (Munich, Germany). ISTH2020 (sequence TTTGTTTACACTTCC) and ISTH2023 (sequence GAGTTTTTCCTTAGG) represent

fully phosphorothioate locked nucleic acid (LNA)-modified antisense oligonucleotides (Supplementary Figure 1). For overexpression of *TGF-β3*, a plasmid containing an untagged human cDNA clone of *TGF-β3* (NM_003239) transfected in a pCMV6-XL5 vector was used (SC118071, Origene, Rockville, MD). Lipofection-based transfections were done with Lipofectamine RNAimax and Opti-MEM (Invitrogen).

Transfections

For lipofection-aided transfections, LTC were transfected at subconfluent conditions in serum-containing medium at a density of 75 000 cells/cm^2 by adding a transfection mix of transfection reagent and oligonucleotides prepared in Opti-MEM medium. After 12-24 h cells were washed and exposed to serum-free medium for 24-120 h as indicated.

For gymnotic transfections, no transfection reagent was used. LTC were seeded at low densities (13 000 cells/cm^2) and treated after 6-12 h with the indicated concentrations of oligonucleotide in full serum-containing medium. On the 3rd day after seeding, full medium supplemented with oligonucleotide was renewed. On the 7th day, medium was removed and the cells were exposed to serum-free-medium.

Trypan blue exclusion assay

Cells were seeded and transfected as described. To obtain counts for dead and viable cells, cell culture supernatant was removed, cells were detached and counted including the cells of the supernatant in an automatic trypan blue-based cell counter (Vi-Cell, Beckman Coulter Inc, Brea, CA) in 3 or 4 replicates.

Immunoblot

Supernatants were generated in serum-free medium after the indicated time points and centrifuged to remove cellular debris. Supernatants were concentrated using a centrifugal filter device (3 kD cut-off, Millipore, Eschborn, Germany). Whole cell lysate preparation and quantification of protein levels were performed as previously described (23). After SDS-PAGE under reducing conditions, proteins were transferred to nitrocellulose membranes (Biorad, Munich, Germany) and blocked in Tris-buffered saline containing 5% skim milk and 0.1% Tween 20 following antibody incubation (antibody information see supplementary methods).
Visualization of protein bands was performed with horseradish peroxidase (HRP)-coupled secondary antibodies (Santa Cruz Biotechnology) and enhanced chemoluminescence (Pierce/Thermo Fisher, Madison, WI). Quantification of bands for correlation analyses was done using ImageJ software (Open Source).

Real-time PCR

mRNA extraction was done using the NucleoSpin® RNA II system (Macherey-Nagel, Düren, Germany) including DNase treatment. cDNA was prepared using a cDNA reverse transcription kit (Applied Biosystems, Forster City, CA).
Gene expression was determined via real-time PCR (23) using ADP-ribosylation factor 1 (ARF-1) as a housekeeping gene with the ΔC_{TT}-method for relative quantification. Primer sequences are indicated in the supplementary material section.

Invasion

For invasion assays, glioma spheroids were generated by incubating 1,500 cells for 72 h in full medium in 96-well plates precoated with 1% Noble Agar (Becton Dickinson, Franklin Lakes, NJ). Thereafter, spheroids were embedded into a collagen matrix containing collagen type I (Corning, NY) in full medium at neutral pH in a 96-

well plate. Sprouting of spheroids was monitored by photographs. For quantification, the median invaded distance of 30 cells was assessed using ImageJ software. The spheroid margin at the corresponding time point was used as a reference for measurement of the invaded distance of sprouting cells.

Animal studies and histology

In vivo studies were performed as previously described (25). In brief, VM/Dk mice (Charles River, Sulzfeld, Germany) were stereotactically implanted into the right striatum with 5 x 10^3 SMA glioma cells, C57Bl/6 mice with 2 x 10^4 GL-261 cells and immunodeficient Crl:CD1-*Foxn1*^{nu} nude mice (Charles River) with 10^5 cells human LN-308 glioma cells in a volume of 2 µl of phosphate-buffered saline (Gibco, Life Technologies). Animal studies were approved by Cantonal Veterinary Office Zurich and Federal Food Safety and Veterinary Office (Permission number 202/2012). For *ex vivo* expression analyses without systemic treatment, the tumor or the non-tumor bearing left hemisphere, considered as “normal brain”, were subjected to mRNA extraction on day 12 after implantation.

Systemic treatment with oligonucleotides was performed by subcutaneous injections as indicated. Brains were collected upon euthanization, embedded in cryomoulds in Shandon Cytochrome yellow (Thermo Scientific, Waltham, MA) and frozen. For histology, brains were cut in 8 µm sections using a Microm HM560 (Microchom HM560, Thermo Scientific) and every 20th section was stained with hematoxylin and eosin (H&E) (25). Tumor volumes were determined using an approximation based on ellipsoid geometric primitive (26). For analysis of invasiveness *in vivo*, we counted satellite lesions as defined by tumor cell aggregates >10 cells at least 3 cell layers distant from the main tumor bulk on all H&E-stained sections.

Database interrogations

The Cancer Genome Atlas (TCGA) database and the R2 microarray analysis and visualization platform (http://hgserver1.amc.nl/cgi-bin/r2/main.cgi#, available on 26th of February) were used to perform survival analyses within the glioblastoma data set containing gene expression data.

Statistical analysis

Representative experiments, commonly performed three times with similar results, are shown. Statistical calculations were done using the software of GraphPad Prism Version 5 (San Diego, CA) including two-sided unpaired t-test (comparison of two groups), one-way ANOVA and Bonferroni post-hoc testing (multiple comparisons) and Spearman correlation coefficient for correlation analyses. A p-value of 0.05 was considered statistically significant.

Results

High TGF-β3 expression is associated with poor survival in glioblastoma

To assess whether *TGF-β3* expression correlates with survival, we used the database of the Cancer Genome Atlas (TCGA) containing data on mRNA expression levels and clinical course of more than 500 patients with glioblastoma. High *TGF-β3* expression was associated with poor survival (13). We next asked whether this association varies within the molecular subtypes classified by Verhaak and colleagues (17). Stratifying patients into these subgroups, data of 82 patients with tumors of the neural, 88 of the proneural, 146 of the mesenchymal and 142 of the classic subtype were available (Supplementary Figure 2). Notably, in the group of the neural subtype the survival benefit for patients with lower *TGF-β3* mRNA expression was highly significant. This was true both when segregating groups into high and low

expression using the cut-off resulting in the highest association (p=0.01, Supplementary Figure 2A) and when using the median expression level as cut-off (p=0.003) (Supplementary Figure 2B).

TGF-β3 is expressed on mRNA and protein level in glioma cell lines

We next characterized our panel of 14 human glioma cell lines (9 LTC, 5 GIC) and 4 murine glioma cell lines for TGF-β3 expression. *TGF-β3* mRNA was expressed in all human cell lines without apparent differences between LTC and GIC (Figure 1A). *TGF-β3* mRNA expression levels were much lower than those of *TGF-β1* or *TGF-β2* in 8 of 9 LTC whereas GIC did not show this pattern (Supplementary Figure 3A, data on human *TGF-β1,2* mRNA been published previously (23)). Murine cell lines expressed *TGF-β3* mRNA, too (Figure 1B). For the murine cell lines, we further assessed the expression levels *ex vivo*, i.e. we implanted the cells orthotopically in syngeneic mice and extracted mRNA from the non-tumor-bearing left hemisphere considered as normal brain and from the tumor after removal from the right hemisphere. Mean levels of *TGF-β3* mRNA in tumoral *ex vivo* samples were more than 3-fold higher in SMA-540 and SMA-560, comparable in GL-261 and more than 5-fold lower in SMA-497 compared to normal brain (Figure 1C). SMA-497 showed the highest mRNA expression *in vitro*, but the lowest *ex vivo*. Comparing all *TGF-β* isoforms *in vitro*, *TGF-β1* was the predominant isoform in SMA-540 and SMA-560, while no significant difference between the isoforms was detected in SMA-497 and GL-261. *Ex vivo,* both *TGF-β1 and TGF-β3* were preferentially expressed in SMA-560, *TGF-β3* was higher than *TGF-β2* in SMA-540 while in line with the expression profile *in vitro*, SMA-497 and GL-261 did not show significant differences between the isoforms (Supplementary Figure 3 B,C, data on murine *TGF-β1,2* mRNA expression have been published previously (27)).

We next analyzed TGF-β3 protein levels in whole cell lysates and cell culture supernatants which turned out to be challenging. The best antibody we identified (ab15537) still had some cross-reactivity with TGF-β2 as assessed by immunoblot loaded with recombinant TGF-β1/2 (Supplementary Figure 4). Still, we considered the detected protein bands as a valid signal since treatment with TGF-β3-specific oligonucleotides reduced the bands at 50 kDa and 12.5 kDa, the presumable pro-form and active form of TGF-β3. Further, these bands increased upon overexpression of TGF-β3 (Figure 1D). In whole cell lysates, the pro-form of TGF-β3, but not the active form, was detected in all cell lines, with the highest levels in T98G, U87MG and LN-308 among LTC, and in T-325 among GIC (Figure 1E). In cell culture supernatants, the pro-form and the active forms of TGF-β3 were detected, with highest levels in LN-428 and T98G, and lower levels in GIC (Figure 1F). TGF-β3 mRNA levels neither correlated with TGF-β3 protein in whole cell lysates nor in the supernatant. However, in the cell culture supernatants, TGF-β3 proform levels correlated with its active form (r=0.64, p=0.01).

In whole cell lysates of mouse glioma cells, the levels of the pro-form of TGF-β3 were similar while levels of the active form were again not detected (Figure 1G). In cell culture supernatants, SMA-497 showed the highest levels of TGF-β3 (pro- and active form) with low levels of active TGF-β3 in the other cell lines (Figure 1H).

Stimulation with different TGF-β isoforms does not disclose isoform-specific effects for pSMAD2

We next confirmed the responsiveness to exogenous TGF-β with regard to isotype-specific functions at the level of canonical signalling. LN-18, U87MG, T98G, LN-308 or LN-229 cells were exposed to increasing concentrations of TGF-β1/2/3. All cell lines

showed a concentration-dependent induction of pSMAD2 by all TGF-β isoforms (Figure 1I). No isoform-specific effect was identified.

TGF-β3-targeted oligonucleotides specifically down-regulate TGF-β3 mRNA in a time- and concentration-dependent manner

We next analysed the activity and specificity of TGF-β3-targeted oligonucleotides (ISTH2020 and ISTH2023) in the human LTC LN-308 characterized by high endogenous TGF-β1 and TGF-β2 levels and high constitutive pSMAD2 and pSMAD1/5 phosphorylation (23, 28). We applied lipofection-based transfections in a nanomolar range and gymnotic transfection without transfection reagent in a micromolar range. Both oligonucleotides down-regulated *TGF-β3* mRNA in a time- and concentration-dependent manner (Figure 2). Both at 24 h and at 72 h, *TGF-β3* mRNA was reduced by more than 75% at 25 nM of ISTH2020 or ISTH2023 using lipofection-based transfection. Of note, in this model, mRNA levels of *TGF-β1* and *TGF-β2* are more than 100-fold higher than those of *TGF-β3*. *TGF-β1* and *TGF-β2* were not reduced by more than 50% upon treatment with TGF-β3-targeted oligonucleotides (Figure 2A). With the gymnotic transfection method, mimicking the systemic administration of the oligonucleotides *in vivo*, ISTH2020 or ISTH2023 at 5 µM led to more than 95% reduction of *TGF-β3* mRNA at day 6 and more than 80% reduction at day 8 of treatment, without affecting *TGF-β1* or *TGF-β2* mRNA by more than 2-fold (Figure 2B). The effect of the oligonucleotides on *TGF-β3* was concentration-dependent with a reduction of more than 50% of *TGF-β3* mRNA up to 12.5 nM (ISTH2020) and 25 nM (ISTH2023) (Figure 2C) with lipofection and up to 0.6 µM (ISTH2023) with gymnotic treatment (Figure 2D). ISTH2020 and ISTH2023 showed comparable activity in the mouse glioma cell line SMA-560 with up to 60% reduction of *TGF-β3* mRNA at 20 nM at 24 and 96 h after lipofection-aided

transfection (Figure 2E) and up to 90% reduction of *TGF-β3* mRNA with gymnotic transfection at 5 µM on day 6 (Figure 2F). With lipofection-based transfection at 50 nM, there was no effect on cell viability or proliferation between 24 and 96 h after transfection (Supplementary Figure 5A). Similarly, with the gymnotic transfection method at 2.5 µM, there were neither significant effects on cell viability nor proliferation between day 4 and 8 of treatment (Supplementary Figure 5B).

Inhibition of TGF-β3 via oligonucleotides reduces SMAD2 and pSMAD1/5 phosphorylation without affecting TGF-β1 and TGF-β2 levels

We next asked whether treatment with TGF-β3-targeted oligonucleotides affects down-stream signaling. With lipofection, pSMAD2 and pSMAD1/5 levels were time- and concentration-dependently down-regulated by both oligonucleotides (Figure 3A,B). Gymnotic delivery of 2.5 µM ISTH2020 or ISTH2023 reduced pSMAD2 earliest on day 7 with the most pronounced effect on day 8. SMAD1/5 phosphorylation was reduced on day 8 (Figure 3C). The effect on SMAD2 and SMAD1/5 phosphorylation was also concentration-dependent as assessed with ISTH2023, however, lower concentrations than 2.5 µM had no effect on SMAD phosphorylation (Figure 3D). Of note, TGF-β1 and TGF-β2 protein levels in the cell culture supernatant were unaffected after 120 h exposure of oligonucleotides (25 nM) with lipofection-aided transfection (Supplementary Figure 6A) and on day 8 of gymnotic treatment with 2.5 µM (Supplementary Figure 6B). We next extended our analysis to the human LTC T98G, and the murine cell line SMA-560. In T98G and SMA-560 cells, both TGF-β3-targeted oligonucleotides reduced SMAD2 phosphorylation, too (Figure 3E).

TGF-β3 gene silencing reduces invasiveness in vitro

TGF-β isoforms are involved in regulating tumor cell invasiveness (29) and TGF-β3 has been attributed isoform-specific effects in wound healing (8), a process involving cell migration and invasion. We therefore assessed whether inhibition of TGF-β3 affected invasiveness of LN-308 glioma cells. Invasiveness was reduced by silencing of TGF-β3 with either ISTH2020 or ISTH2023 (Figure 4).

TGF-β3-targeted oligonucleotides inhibit SMAD phosphorylation induced by exogenous TGF-β1/2/3

We next asked whether the inhibitory effect on SMAD phosphorylation by TGF-β3-targeted oligonucleotides is preserved upon additional stimulation with other TGF-β isoforms. Surprisingly, SMAD2 and SMAD1/5 phosphorylation were induced less by TGF-β1/2 at 0.5 ng/ml in the presence of TGF-β3-targeted oligonucleotides. This effect still held true for SMAD2 phosphorylation at higher concentrations (5 ng/ml) of TGF-β1 and TGF-β2 (Figure 5).

Inhibition of TGF-β3 in vivo

The TGF-β3-targeted oligonucleotides ISTH2020 and ISTH2023 were shown to exhibit no liver toxicity upon systemic administration as assessed by plasma alanin-transaminase (ALT) in murine models (M. Janicot, unpublished observation). To verify target inhibition *in vivo,* we systemically treated mice bearing syngeneic (SMA-560) or xenograft (LN-308) gliomas with control or ISTH2023 oligonucleotides. Tumors derived from SMA-560 cells showed significantly higher mRNA expression of *TGF-β3* than normal brain. Upon treatment with ISTH2023, tumoral mRNA levels of *TGF-β3* were reduced by more than 30% (Figure 6A). Importantly, *PAI-1* as a transcriptional down-stream target was significantly reduced in ISTH2023-treated

tumors (Figure 6B). Similar to the *in vitro* data, levels of *TGF-β1/2* were not altered by ISTH2023 (Figure 6C).

In the xenograft LN-308 model, ISTH2023 significantly reduced human *TGF-β3* (Figure 6D) and human *PAI-1* (Figure 6E) mRNA levels while tumoral human TGF-β1/2 was not affected significantly (Figure 6F).

We next asked whether treatment with TGF-β3-targeted oligonucleotides affects the phenotype of experimental gliomas *in vivo*. Tumor size as assessed by volumetric measurement of H&E-stained slides was not significantly affected by ISTH2023 either in the SMA-560 (Figure 6G) or in the LN-308 model (Figure 6J). However, a trend towards a reduced tumor size was observed in both models in mice treated with ISTH2023. In the SMA-560 model, we assessed the number of satellite lesions as a morphologic surrogate marker of tumor invasiveness. The mean number of satellite lesions per brain section was 5 in the control group versus 3 in the group treated with ISTH2023. This reduction was not significant (p=0.41) when comparing the mean number of satellites per section of the 4 brains per group, but was significant (p=0.0036) when comparing the results of all H&E-stained brain sections per group (n=149 “control” versus n=148 “ISTH2023”) (Figure 6H, representative images shown in Figure 6I). In the LN-308 model, assessment of satellite lesions was not meaningful since the mean number of satellites per brain section was less than 1 in either group (representative images shown in Figure 6K).

Discussion

The TGF-β pathway has been attributed a key role in the pathogenesis of glioblastoma with regard to immunosuppression, invasion, angiogenesis and maintenance of the stem cell phenotype (30, 31). Pharmacological strategies to

interfere with the TGF-β pathway via inhibition of the kinase activity of TGF-β-receptor type I were promising in murine models, but so far disappointing in the clinic (29, 32-34). A ligand-based approach using AP-12009, an antisense oligonucleotide supposed to target TGF-β2, administered intratumorally, suggested non-inferiority to alkylating chemotherapy in a phase II clinical trial, however, interpretation of the trial results remained controversial (35, 36).

Targeting the ligands rather than their bona fide receptors might have different therapeutic safety, tolerability and efficacy profiles. Beyond AP-12009, a TGF-β2-antisense-modified tumor cell vaccine as another ligand-based approach of targeting the TGF-β pathway in glioblastoma has been tested in the clinic in a phase I trial (37). Targeting TGF-β expression through integrin inhibition has yielded promising results *in vitro* (38) but was not active in glioblastoma patients (39). TGF-β1 and TGF-β2 were considered as the most important isoforms in glioblastoma while little is known on the role of TGF-β3 in the context of glioblastoma (13).

Here, we present a comprehensive analysis of TGF-β3 mRNA and protein expression in human and murine *in vitro* models and show that *TGF-β3* expression can be specifically inhibited by oligonucleotides *in vitro* and *in vivo.* This inhibition led to down-regulation of SMAD signaling *in vitro* and of the SMAD-dependent target gene *PAI-1 in vivo* despite the presence of TGF-β1 and TGF-β2.

The fact that high *TGF-β3* mRNA expression correlates with poor survival in glioblastoma patients in the TCGA database (13) suggests targeting of TGF-β3 as a promising strategy. A previous study performed using the Rembrandt database showed that expression levels of more than 2-fold of *TGF-β1* (p=0.02) or more than 5-fold of *TGF-β2* (p=0.05) correlated with poor survival while more than 2-fold expression of *TGF-β3* was without prognostic significance (p=0.08) (16). Divergent

results regarding a prognostic role of *TGF-β3* expression might be due to different samples in the respective databases with tumors exhibiting genetic heterogeneity or the use of different cut-offs. This would be in line with our observation that the association of *TGF-β3* mRNA expression with poor survival is most prominent in the neural subtype of the Verhaak classification (Supplementary Figure 2). These data suggest that therapeutic targeting of *TGF-β3* might be most effective in these tumors.

We show that *TGF-β3* expression in human glioma cell lines is less abundant than that of *TGF-β1* and *TGF-β2*, in line with a previous study based on glioblastoma tissue samples (13), however, GIC did not show this pattern (Supplementary Figure 3A). Intracellular protein levels of TGF-β3 were detected in all human and murine cell lines while the 12.5 kDa secreted form of TGF-β3 was present in the majority of human LTC, but not GIC (Figure 1D-F). This might reflect a different importance of this isoform in these cell types. All three TGF-β isoforms induced SMAD2 phosphorylation in a concentration-dependent manner (Figure 1I), not revealing isoform-specific differences. However, specific time- and concentration-dependent inhibition of endogenous TGF-β3 by oligonucleotides (Figure 2) reduced SMAD2 and SMAD1/5 phosphorylation despite the concurrent presence of TGF-β1/2 which would be expected to be major and sufficient drivers of baseline phosphorylation levels (Figure 3). The gymnotic transfection method with omission of transfection reagent and micromolar concentrations intends to mimic the systemic administration of the drug *in vivo* and led to a similarly effective inhibition of *TGF-β3* expression and reduction of SMAD2 and SMAD1/5 phosphorylation as the conventional lipofection-based transfection method (Figures 2,3).

The profound effect of inhibition of TGF-β3 on SMAD phosphorylation, albeit expressed at mRNA levels much lower than those of TGF-β1/2 in these cells,

suggests a major distinct regulatory role of this isoform. The reduction in phosphorylated SMAD levels by inhibition of TGF-β3 leading to reduced invasiveness in the LN-308 model (Figure 4) points towards biological and clinical relevance of targeting TGF-β3 in glioblastoma.

The hypothesis that TGF-β3 might exert major biological effects despite its low expression levels and concurrent presence of the other TGF-β isoforms is further supported by our observation that TGF-β3-specific oligonucleotides reduce SMAD phosphorylation even in the presence of exogenous TGF-β1/2 (Figure 5). For the three TGF-β isoforms, auto-feedback loops inducing their own expression mediated by different transcription factors according to the respective isoform with differential promotor regions have been suggested (16, 40, 41). An impaired auto-feedback loop through resulting from TGF-β3 depletion might explain the profound effects on SMAD phosphorylation despite the presence of the other isoforms. TGF-β3-dependent epithelial-mesenchymal transition is downstream of a TGF-β1- and TGF-β2-induced upregulation of the E-cadherin repressors snail and slug (42), supporting the concept of hierarchical importance of the different isoforms. Potentially, TGF-β3 functions as a gatekeeper controlling down-stream signaling despite high expression of TGF-β1 and TGF-β2 isoforms.

Treatment with the TGF-β3-specific oligonucleotides *in vivo* also resulted in specific target down-regulation without significant effects on the other TGF-β isoforms. Biological relevance of reduced TGF-β3 levels was demonstrated by profound down-regulation of the SMAD-dependent target gene *PAI-1* both in the syngeneic SMA-560 and xenograft LN-308 model (Figure 6). Short-term inhibition of TGF-β3 *in vivo* showed only a minor, non-significant reduction of tumor volumes (Figure 6), in line with the observation that there are no significant effects on cell viability nor

proliferation *in vitro* (Supplementary Figure 5). Reduced TGF-β3 levels were associated with a minor reduction of tumor invasiveness *in vivo* (Figure 6), but prolonged exposure to inhibitors is probably necessary for more prominent effects. Further, inhibition of TGF-β3 alone might not be sufficient to block tumor invasiveness, given the complexity *in vivo* involving other drivers of tumor invasion and potential escape mechanisms.

In summary, we demonstrate that isoform-specific targeting of TGF-β3 is feasible and effective by subcutaneous injection of a suitable oligonucleotide.

Pharmacological inhibition of TGF-β3 in glioblastoma may therefore represent a promising strategy warranting further investigation.

Acknowledgement: The authors thank Monika Kruszyńska for her expert technical assistance.

References

1. Hinck AP, Archer SJ, Qian SW, Roberts AB, Sporn MB, Weatherbee JA, et al. Transforming growth factor beta 1: three-dimensional structure in solution and comparison with the X-ray structure of transforming growth factor beta 2. Biochemistry. 1996;35:8517-34.

2. Bocharov EV, Blommers MJ, Kuhla J, Arvinte T, Burgi R, Arseniev AS. Sequence-specific 1H and 15N assignment and secondary structure of transforming growth factor beta3. J Biomol NMR. 2000;16:179-80.

3. Hart PJ, Deep S, Taylor AB, Shu Z, Hinck CS, Hinck AP. Crystal structure of the human TbetaR2 ectodomain--TGF-beta3 complex. Nat Struct Biol. 2002;9:203-8.

4. Grutter C, Wilkinson T, Turner R, Podichetty S, Finch D, McCourt M, et al. A cytokine-neutralizing antibody as a structural mimetic of 2 receptor interactions. Proc Natl Acad Sci U S A. 2008;105:20251-6.

5. Laverty HG, Wakefield LM, Occleston NL, O'Kane S, Ferguson MW. TGF-beta3 and cancer: a review. Cytokine Growth Factor Rev. 2009;20:305-17.

6. Taya Y, O'Kane S, Ferguson MW. Pathogenesis of cleft palate in TGF-beta3 knockout mice. Development. 1999;126:3869-79.

7. Yang LT, Kaartinen V. Tgfb1 expressed in the Tgfb3 locus partially rescues the cleft palate phenotype of Tgfb3 null mutants. Dev Biol. 2007;312:384-95.

8. Shah M, Foreman DM, Ferguson MW. Neutralisation of TGF-beta 1 and TGF-beta 2 or exogenous addition of TGF-beta 3 to cutaneous rat wounds reduces scarring. J Cell Sci. 1995;108 (Pt 3):985-1002.

9. Kaartinen V, Voncken JW, Shuler C, Warburton D, Bu D, Heisterkamp N, et al. Abnormal lung development and cleft palate in mice lacking TGF-beta 3 indicates defects of epithelial-mesenchymal interaction. Nat Genet. 1995;11:415-21.

10. Dickson MC, Martin JS, Cousins FM, Kulkarni AB, Karlsson S, Akhurst RJ. Defective haematopoiesis and vasculogenesis in transforming growth factor-beta 1 knock out mice. Development. 1995;121:1845-54.

11. Sanford LP, Ormsby I, Gittenberger-de Groot AC, Sariola H, Friedman R, Boivin GP, et al. TGFbeta2 knockout mice have multiple developmental defects that are non-overlapping with other TGFbeta knockout phenotypes. Development. 1997;124:2659-70.

12. Kjellman C, Olofsson SP, Hansson O, Von Schantz T, Lindvall M, Nilsson I, et al. Expression of TGF-beta isoforms, TGF-beta receptors, and SMAD molecules at different stages of human glioma. Int J Cancer. 2000;89:251-8.

13. Frei K, Gramatzki D, Tritschler I, Schroeder JJ, Espinoza L, Rushing EJ, et al. Transforming growth factor-beta pathway activity in glioblastoma. Oncotarget. 2015;6:5963-77.

14. Friese MA, Wischhusen J, Wick W, Weiler M, Eisele G, Steinle A, et al. RNA interference targeting transforming growth factor-beta enhances NKG2D-mediated antiglioma immune response, inhibits glioma cell migration and invasiveness, and abrogates tumorigenicity in vivo. Cancer Res. 2004;64:7596-603.

15. Eisele G, Wischhusen J, Mittelbronn M, Meyermann R, Waldhauer I, Steinle A, et al. TGF-beta and metalloproteinases differentially suppress NKG2D ligand surface expression on malignant glioma cells. Brain. 2006;129:2416-25.

16. Rodon L, Gonzalez-Junca A, Inda Mdel M, Sala-Hojman A, Martinez-Saez E, Seoane J. Active CREB1 promotes a malignant TGFbeta2 autocrine loop in glioblastoma. Cancer Discov. 2014;4:1230-41.

17. Verhaak RG, Hoadley KA, Purdom E, Wang V, Qi Y, Wilkerson MD, et al. Integrated genomic analysis identifies clinically relevant subtypes of glioblastoma

characterized by abnormalities in PDGFRA, IDH1, EGFR, and NF1. Cancer Cell. 2010;17:98-110.

18. Weller M, Rieger J, Grimmel C, Van Meir EG, De Tribolet N, Krajewski S, et al. Predicting chemoresistance in human malignant glioma cells: the role of molecular genetic analyses. Int J Cancer. 1998;79:640-4.

19. Fraser H. Astrocytomas in an inbred mouse strain. J Pathol. 1971;103:266-70.

20. Sampson JH, Ashley DM, Archer GE, Fuchs HE, Dranoff G, Hale LP, et al. Characterization of a spontaneous murine astrocytoma and abrogation of its tumorigenicity by cytokine secretion. Neurosurgery. 1997;41:1365-72; discussion 72-3.

21. Ahmad M, Frei K, Willscher E, Stefanski A, Kaulich K, Roth P, et al. How stemlike are sphere cultures from long-term cancer cell lines? Lessons from mouse glioma models. J Neuropathol Exp Neurol. 2014;73:1062-77.

22. Weiler M, Blaes J, Pusch S, Sahm F, Czabanka M, Luger S, et al. mTOR target NDRG1 confers MGMT-dependent resistance to alkylating chemotherapy. Proc Natl Acad Sci U S A. 2014;111:409-14.

23. Seystahl K, Tritschler I, Szabo E, Tabatabai G, Weller M. Differential regulation of TGF-beta-induced, ALK-5-mediated VEGF release by SMAD2/3 versus SMAD1/5/8 signaling in glioblastoma. Neuro Oncol. 2015;17:254-65.

24. Rieger J, Lemke D, Maurer G, Weiler M, Frank B, Tabatabai G, et al. Enzastaurin-induced apoptosis in glioma cells is caspase-dependent and inhibited by BCL-XL. J Neurochem. 2008;106:2436-48.

25. Szabo E, Schneider H, Seystahl K, Rushing EJ, Herting F, Weidner KM, et al. Autocrine VEGFR1 and VEGFR2 signaling promotes survival in human glioblastoma models in vitro and in vivo. Neuro Oncol. 2016;18:1242-52.

26. Schmidt KF, Ziu M, Schmidt NO, Vaghasia P, Cargioli TG, Doshi S, et al. Volume reconstruction techniques improve the correlation between histological and in vivo tumor volume measurements in mouse models of human gliomas. J Neurooncol. 2004;68:207-15.

27. Mangani D, Weller M, Seyed Sadr E, Willscher E, Seystahl K, Reifenberger G, et al. Limited role for transforming growth factor-beta pathway activation-mediated escape from VEGF inhibition in murine glioma models. Neuro Oncol. 2016;18:1610-21.

28. Leitlein J, Aulwurm S, Waltereit R, Naumann U, Wagenknecht B, Garten W, et al. Processing of immunosuppressive pro-TGF-beta 1,2 by human glioblastoma cells involves cytoplasmic and secreted furin-like proteases. J Immunol. 2001;166:7238-43.

29. Uhl M, Aulwurm S, Wischhusen J, Weiler M, Ma JY, Almirez R, et al. SD-208, a novel transforming growth factor beta receptor I kinase inhibitor, inhibits growth and invasiveness and enhances immunogenicity of murine and human glioma cells in vitro and in vivo. Cancer Res. 2004;64:7954-61.

30. Seoane J. TGFbeta and cancer initiating cells. Cell Cycle. 2009;8:3787-8.

31. Weller M, Fontana A. The failure of current immunotherapy for malignant glioma. Tumor-derived TGF-beta, T-cell apoptosis, and the immune privilege of the brain. Brain Res Brain Res Rev. 1995;21:128-51.

32. Tran TT, Uhl M, Ma JY, Janssen L, Sriram V, Aulwurm S, et al. Inhibiting TGF-beta signaling restores immune surveillance in the SMA-560 glioma model. Neuro Oncol. 2007;9:259-70.

33. Rodon J, Carducci MA, Sepulveda-Sanchez JM, Azaro A, Calvo E, Seoane J, et al. First-in-human dose study of the novel transforming growth factor-beta receptor

I kinase inhibitor LY2157299 monohydrate in patients with advanced cancer and glioma. Clin Cancer Res. 2015;21:553-60.

34. Brandes AA, Carpentier AF, Kesari S, Sepulveda-Sanchez JM, Wheeler HR, Chinot O, et al. A phase II randomized study of galunisertib monotherapy or galunisertib plus lomustine compared with lomustine monotherapy in patients with recurrent glioblastoma. Neuro Oncol. 2016.

35. Bogdahn U, Hau P, Stockhammer G, Venkataramana NK, Mahapatra AK, Suri A, et al. Targeted therapy for high-grade glioma with the TGF-beta2 inhibitor trabedersen: results of a randomized and controlled phase IIb study. Neuro Oncol. 2011;13:132-42.

36. Wick W, Weller M. Trabedersen to target transforming growth factor-beta: when the journey is not the reward, in reference to Bogdahn et al. (Neuro-Oncology 2011;13:132-142). Neuro Oncol. 2011;13:559-60; author reply 61-2.

37. Fakhrai H, Mantil JC, Liu L, Nicholson GL, Murphy-Satter CS, Ruppert J, et al. Phase I clinical trial of a TGF-beta antisense-modified tumor cell vaccine in patients with advanced glioma. Cancer Gene Ther. 2006;13:1052-60.

38. Roth P, Silginer M, Goodman SL, Hasenbach K, Thies S, Maurer G, et al. Integrin control of the transforming growth factor-beta pathway in glioblastoma. Brain. 2013;136:564-76.

39. Stupp R, Hegi ME, Gorlia T, Erridge SC, Perry J, Hong YK, et al. Cilengitide combined with standard treatment for patients with newly diagnosed glioblastoma with methylated MGMT promoter (CENTRIC EORTC 26071-22072 study): a multicentre, randomised, open-label, phase 3 trial. Lancet Oncol. 2014;15:1100-8.

40. Liu GM, Ding W, Neiman J, Mulder KM. Requirement of Smad3 and CREB-1 in mediating transforming growth factor-beta (TGF beta) induction of TGF beta 3 secretion. J Biol Chem. 2006;281:29479-90.

41. Yue JB, Mulder KM. Requirement of Ras/MAPK pathway activation by transforming growth factor beta for transforming growth factor beta-1 production in a Smad-dependent pathway. J Biol Chem. 2000;275:35656.

42. Medici D, Hay ED, Olsen BR. Snail and Slug promote epithelial-mesenchymal transition through beta-catenin-T-cell factor-4-dependent expression of transforming growth factor-beta3. Mol Biol Cell. 2008;19:4875-87.

Figure Legends

Figure 1. *TGF-β3* mRNA expression and TGF-β3 protein levels in glioma cell lines.

A-C. The expression of *TGF-β3* mRNA in human (A) and murine cell lines *in vitro* (B) and *ex vivo* (C) was assessed by RT-PCR. As a control for *ex vivo* samples, expression levels of normal syngeneic mouse brain (NB) were included. Results are expressed as means and SD (n=3 independent samples, except D-247MG with n=1; n=1 for NB). D-H. TGF-β3 protein levels were assessed by immunoblot. The specificity of the bands was verified by lipofection-based transfection with TGF-β3-targeted antisense oligonucleotides in whole cell lysates of human LN-308 and murine SMA-560 cells (control versus ISTH2020 or ISTH2023 at 50 nM collected at 96 h after transfection for LN-308 and at 25 nM collected 72 h after transfection for SMA-560) and in supernatants of LN-308 cells (collected 96 h after transfection with control, ISTH2020 or ISTH2023 at 50 nM) and in supernatants of LN-18 cells (empty vector versus genetic overexpression of *TGF-β3*) (D). TGF-β3 protein levels were examined in cell lysates (E, G) and cell culture supernatants (F, H) of human (E, F) and murine cell lines (G,H) by immunoblot and quantification of bands by densitometric analyses using ImageJ. I. LN-18, U87MG, T98G, LN-308 or LN-229 cells were stimulated with TGF-β1/2/3 at 0.1, 1 or 10 ng for 24 h. Whole cell lysates were analysed for pSMAD2. Actin, GAPDH (cell lysates) or Ponceau (supernatants) served as loading controls.

Figure 2. Specific down-regulation of TGF-β3 mRNA by oligonucleotides.

A-D. *TGF-β1,2,3* mRNA expression was analysed by RT-PCR in LN-308 cells after treatment with control or TGF-β3-targeted oligonucleotides ISTH2020 or ISTH2023

via lipofection at 25 nM after 24 h or 72 h (A) or via gymnotic transfection after 6 and 8 days at 5 µM (B), at 12.5, 25 or 50 nM after 24 h via lipofection (C) and at 0.3, 0.6, 1.3, 2.5 or 5 µM after 8 days (D). Data shown in C and D were normalized to corresponding control. E,F. SMA-560 cells were analyzed for *TGF-β3* mRNA expression after transfection with control or TGF-β3-targeted oligonucleotides via lipofection (E, 24 h or 96 h at 5 or 20 nM) or gymnotic transfection (F, 5 µM, day 6). Results shown in A-E are expressed as means of representative experiments performed in duplicates.

Figure 3. TGF-β3 gene silencing interferes with down-stream SMAD signaling

A-D. LN-308 cells were transfected with control or ISTH2020 and ISTH2023 via lipofection at 25 nM for 48 h or 120 h (A), at 25, 50 and 100 nM (B) or via gymnotic transfection for 7 and 8 days at 2.5 µM (C), and at 1.3, 2.5 and 5 µM for 8 days (D). pSMAD2, pSMAD1/5, TGF-β3 and actin/GAPDH as loading controls were analysed in whole cell lysates and TGF-β3 in cell culture supernatants (SN) by immunoblot. E. Whole cell lysates of T98G cells harvested 96 h after lipofection with 50 nM of control or TGF-β3-targeted oligonucleotide were analyzed for pSMAD2. SMA-560 cells were treated similarly with 25 nM oligonucleotide, lysates harvested 72h after transfection, and analyzed for pSMAD2. Actin was included as a loading control.

Figure 4. Silencing of TGF-β3 reduces invasiveness *in vitro*.

A. Spheroids of LN-308 cells were generated by incubating 1,500 cells for 72 h in plates precoated with 1% agar, plated in a 3D collagen I matrix and evaluated at baseline (0 h) and after 48, 72 and 96 h (representative images). During spheroid generation and the invasion assay, the cells were exposed to control (left) or oligonucleotide treatment with ISTH2020 (middle) or ISTH2023 (right, gymnotic

delivery, 2.5 µM). B. The invaded area was analysed after the indicated time points (means and SD of a representative experiment performed in n=3 replicates (control, ISTH2023) or n=4 replicates (ISTH2020), one-way-ANOVA and Bonferroni post-hoc tests).

Figure 5. TGF-β3-targeted oligonucleotides inhibit SMAD phosphorylation induced by TGF-β1/2 isoforms. LN-308 cells were transfected with control, ISTH2020 or ISTH2023 oligonucleotides (lipofection, 50 nM) and were stimulated 48 h after transfection with or without TGF-β1/2 at 0.5 ng/ml and 5 ng/ml for 1 h. Whole cell lysates were analysed for pSMAD2, pSMAD1/5 and actin as a loading control.

Figure 6. Inhibition of TGF-β3 by isoform-specific oligonucleotides *in vivo.* A-C. VM/Dk mice, orthotopically implanted with SMA-560 cells, were subcutaneously treated with control or ISTH2023 oligonucleotides at 20 mg/kg body weight for 5 consecutive days, starting on day 5 after implantation. Brains were removed 24 h after the last treatment. Murine *TGF-β3* (A), *PAI-1* (B) or *TGF-β1/2* mRNA (C) levels were assessed by RT-PCR in left hemisphere considered as normal brain (NB) and the tumor-bearing right hemisphere (Tu). Results are expressed as means and SD of n=4 mice per group. D-F. Nude mice, orthotopically implanted with LN-308 cells, were treated as in A-C, but starting on day 30 after implantation for 5 consecutive days. Human *TGF-β3* (D), *PAI-1* (E), or *TGF-β1/2* (F) mRNA levels were assessed as in A-C. G-I. VM/Dk mice, orthotopically implanted with SMA-560 cells, were treated as in A-C followed by 3 injections per week until the first mouse in the experiment developed neurological symptoms. On H&E stained brain sections, tumor volume (G, means and SD of n=4 mice per group) and tumor satellites (H, means and SD of the mean number of satellites per section of n=4 tumors per group (upper panel) and

means and SD of all stained sections (n=149 control versus n=148 ISTH2023, lower panel)) were assessed as described in the methods section; I shows representative images (scale bars correspond to 100 µm). J-K. Nude mice, orthotopically implanted with LN-308 cells, were treated with control or ISTH2023, starting the treatment on day 21 with 5 daily injections followed by 3 injections per week until the first mouse became symptomatic. Tumor volume (J) was assessed as in G and representative images are shown in K (scale bars 100 µm). A-J. Statistics were performed with one-way ANOVA and Bonferroni post-hoc testing in case of multiple comparisons (A-C, F) or t-test (D, E, G, H, J).

Figure 1

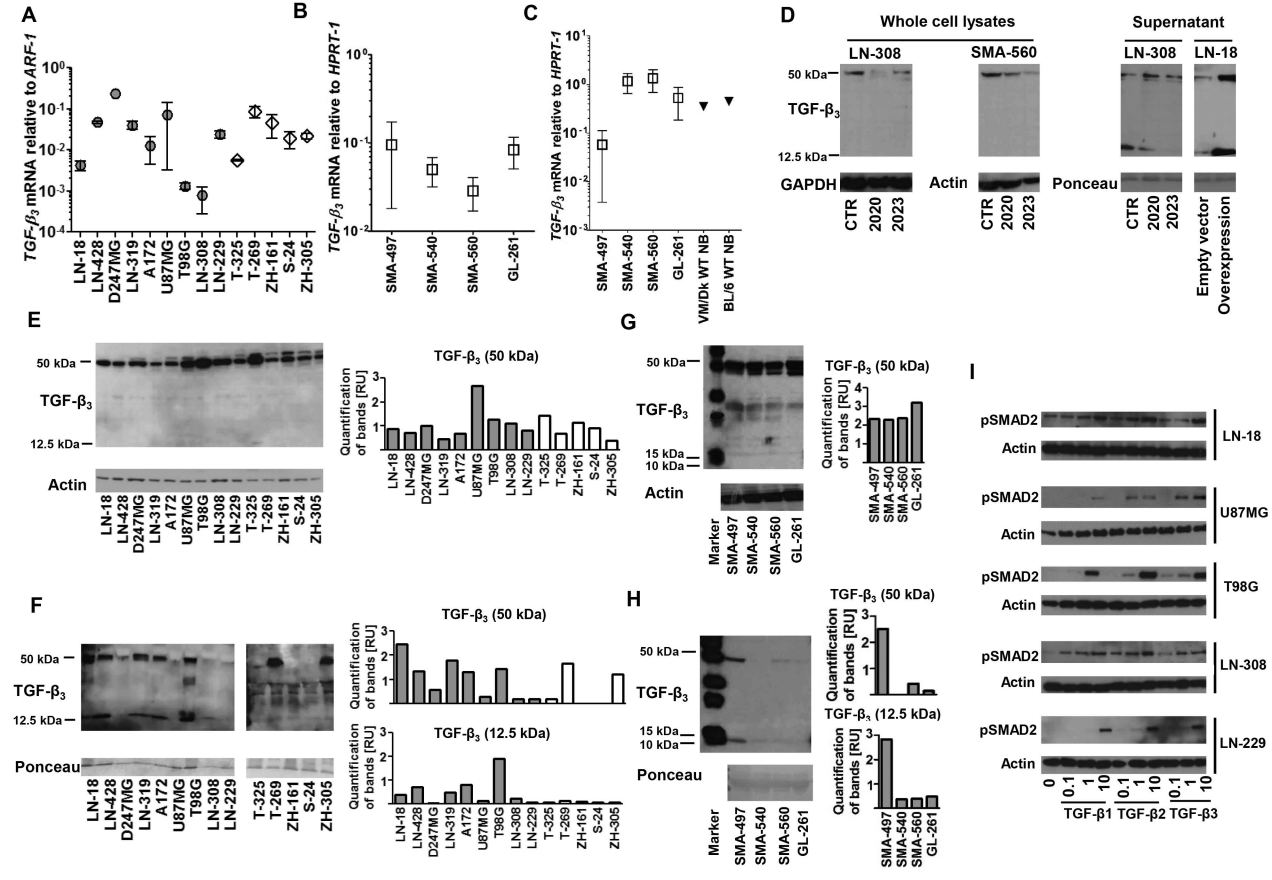
A
B
C
D
E
F
G
H
I
TGF-β3 mRNA relative to ARF-1
TGF-β3 mRNA relative to HPRT-1
LN-18
LN-428
D247MG
LN-319
A172
U87MG
T98G
LN-308
LN-229
T-325
T-269
ZH-161
S-24
ZH-305
SMA-497
SMA-540
SMA-560
GL-261
VM/Dk WT NB
BL/6 WT NB
Whole cell lysates
Supernatant
50 kDa
12.5 kDa
TGF-β3
GAPDH
Actin
Ponceau
CTR
2020
2023
Empty vector
Overexpression
TGF-β3 (50 kDa)
TGF-β3 (12.5 kDa)
Quantification of bands [RU]
15 kDa
10 kDa
Marker
pSMAD2
TGF-β1
TGF-β2
TGF-β3

Figure 2

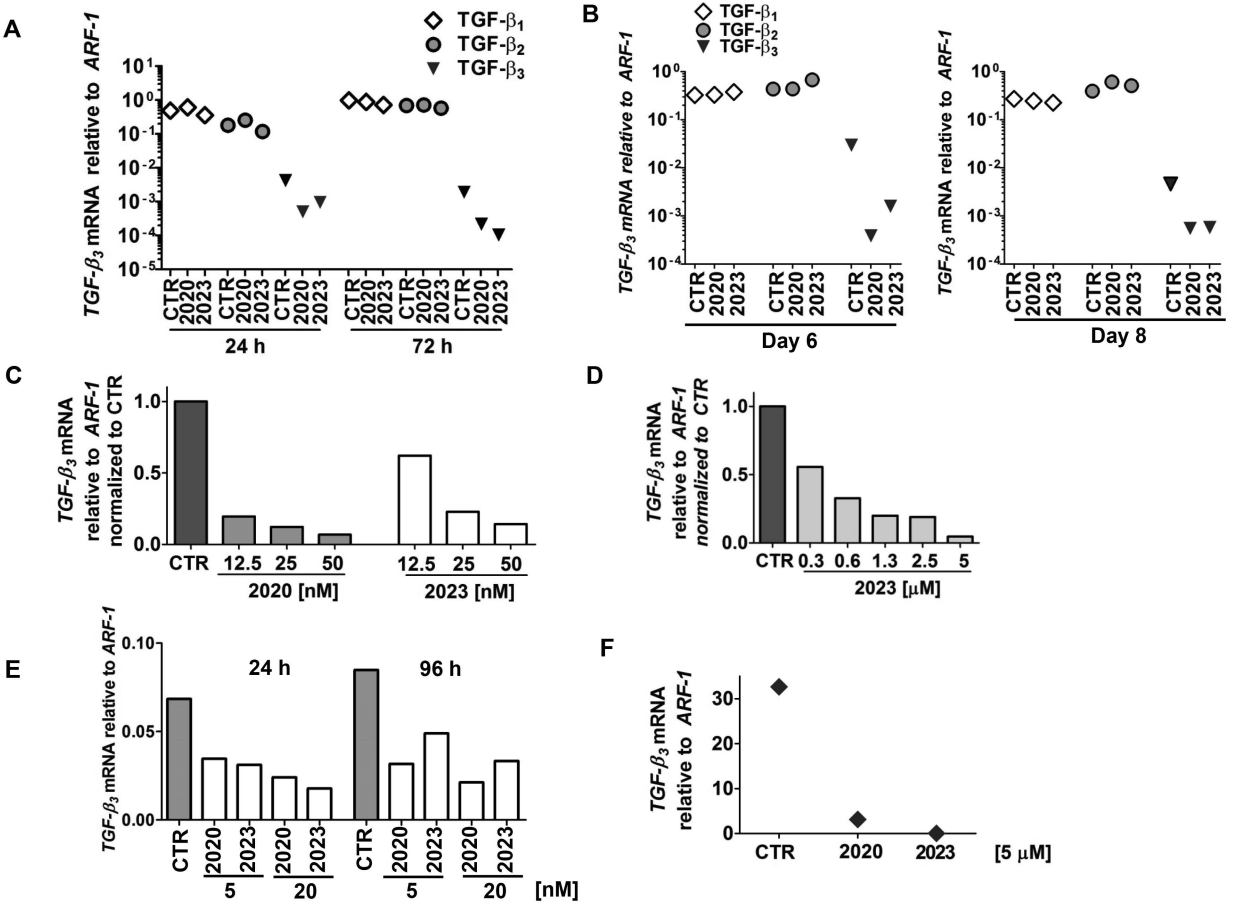
A
TGF-β1
TGF-β2
TGF-β3
TGF-β3 mRNA relative to ARF-1
CTR
2020
2023
24 h
72 h
B
TGF-β1
TGF-β2
TGF-β3
TGF-β3 mRNA relative to ARF-1
Day 6
Day 8
C
TGF-β3 mRNA relative to ARF-1 normalized to CTR
CTR
12.5
25
50
2020 [nM]
2023 [nM]
D
TGF-β3 mRNA relative to ARF-1 normalized to CTR
CTR
0.3
0.6
1.3
2.5
5
2023 [μM]
E
TGF-β3 mRNA relative to ARF-1
24 h
96 h
CTR
2020
2023
5
20
[nM]
F
TGF-β3 mRNA relative to ARF-1
CTR
2020
2023
[5 μM]

Figure 3

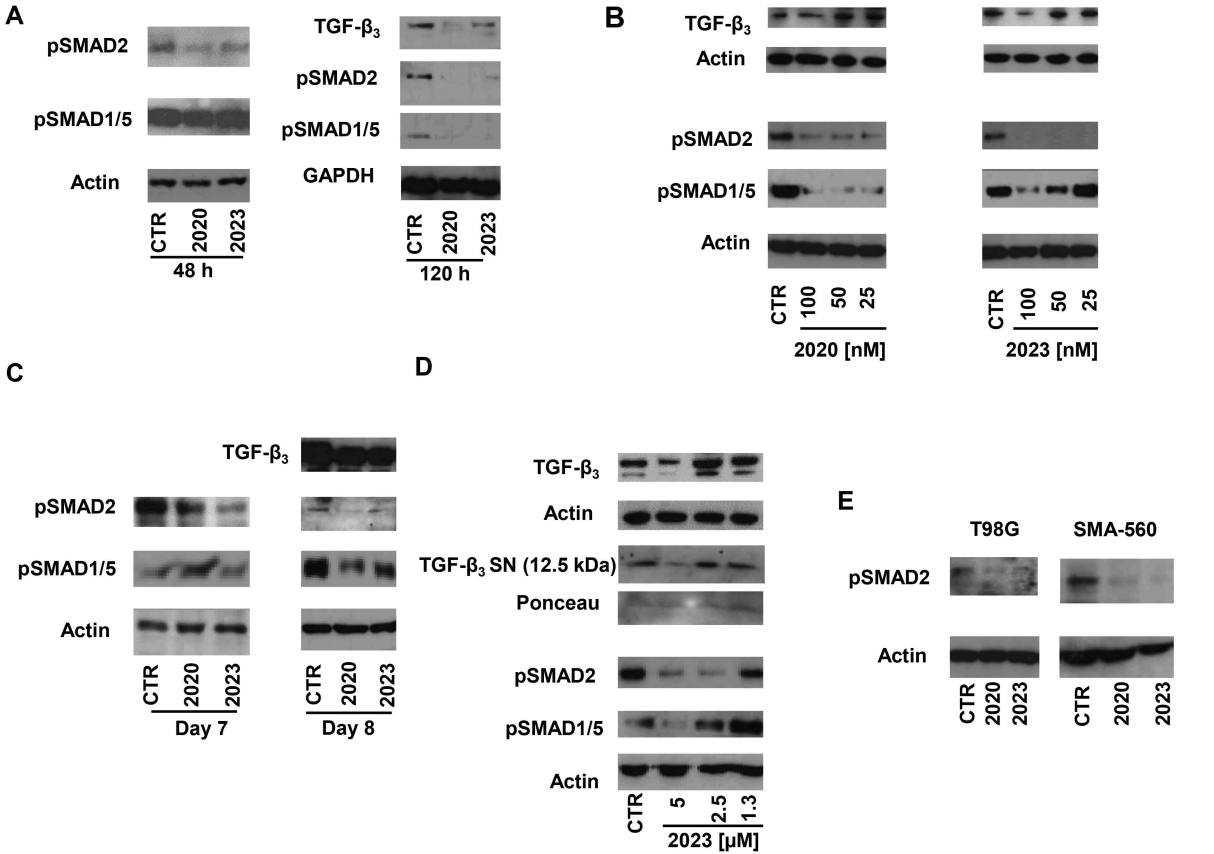
A
pSMAD2
pSMAD1/5
Actin
CTR
2020
2023
48 h
TGF-β3
pSMAD2
pSMAD1/5
GAPDH
CTR
2020
2023
120 h
B
TGF-β3
Actin
pSMAD2
pSMAD1/5
Actin
CTR
100
50
25
2020 [nM]
CTR
100
50
25
2023 [nM]
C
TGF-β3
pSMAD2
pSMAD1/5
Actin
CTR
2020
2023
Day 7
CTR
2020
2023
Day 8
D
TGF-β3
Actin
TGF-β3 SN (12.5 kDa)
Ponceau
pSMAD2
pSMAD1/5
Actin
CTR
5
2.5
1.3
2023 [μM]
E
T98G
SMA-560
pSMAD2
Actin
CTR
2020
2023
CTR
2020
2023

Figure 4

A

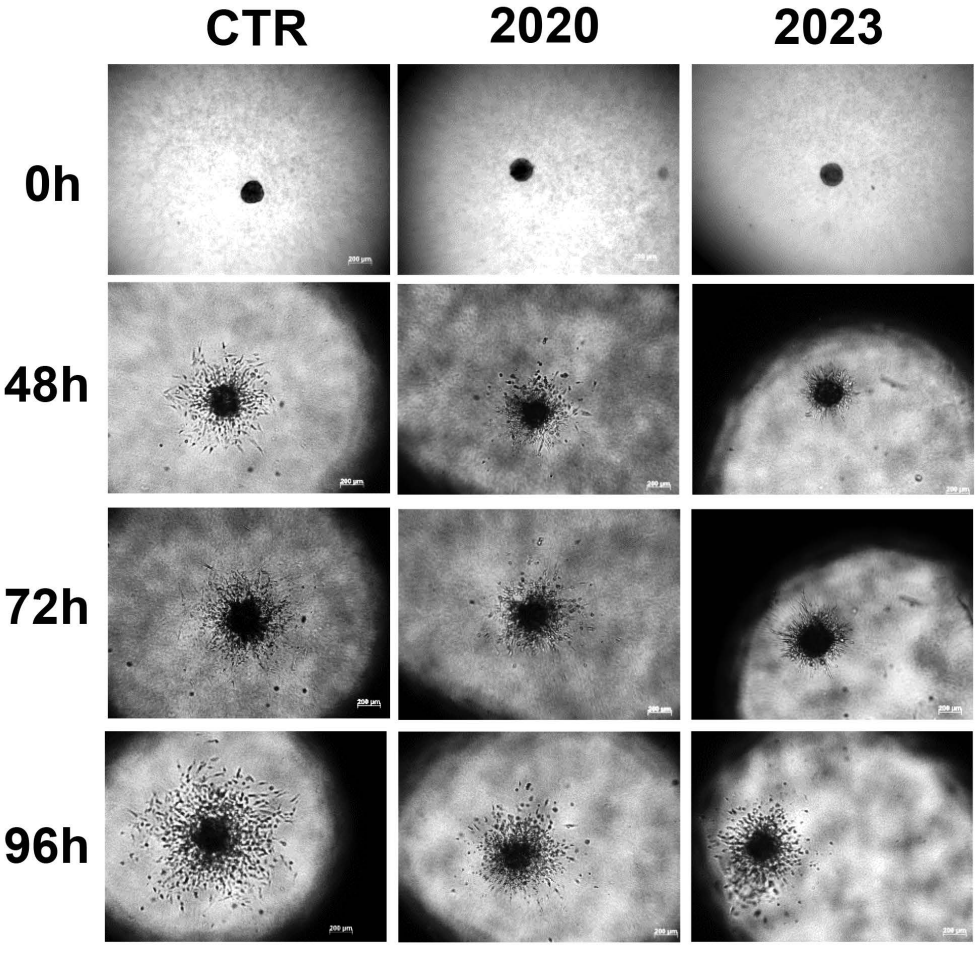
CTR
2020
2023
0h
48h
72h
96h

B

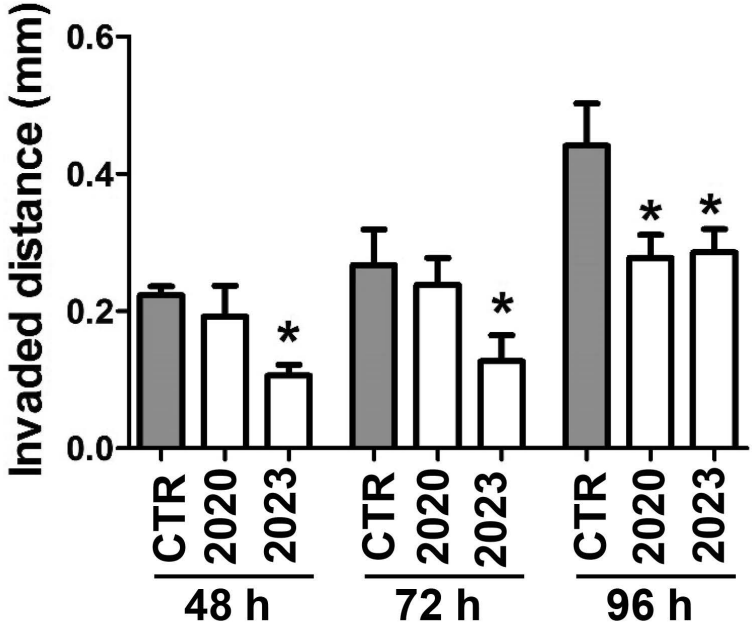
Invaded distance (mm)
0.6
0.4
0.2
0.0
*
*
*
*
*
CTR
2020
2023
CTR
2020
2023
CTR
2020
2023
48 h
72 h
96 h

Figure 5

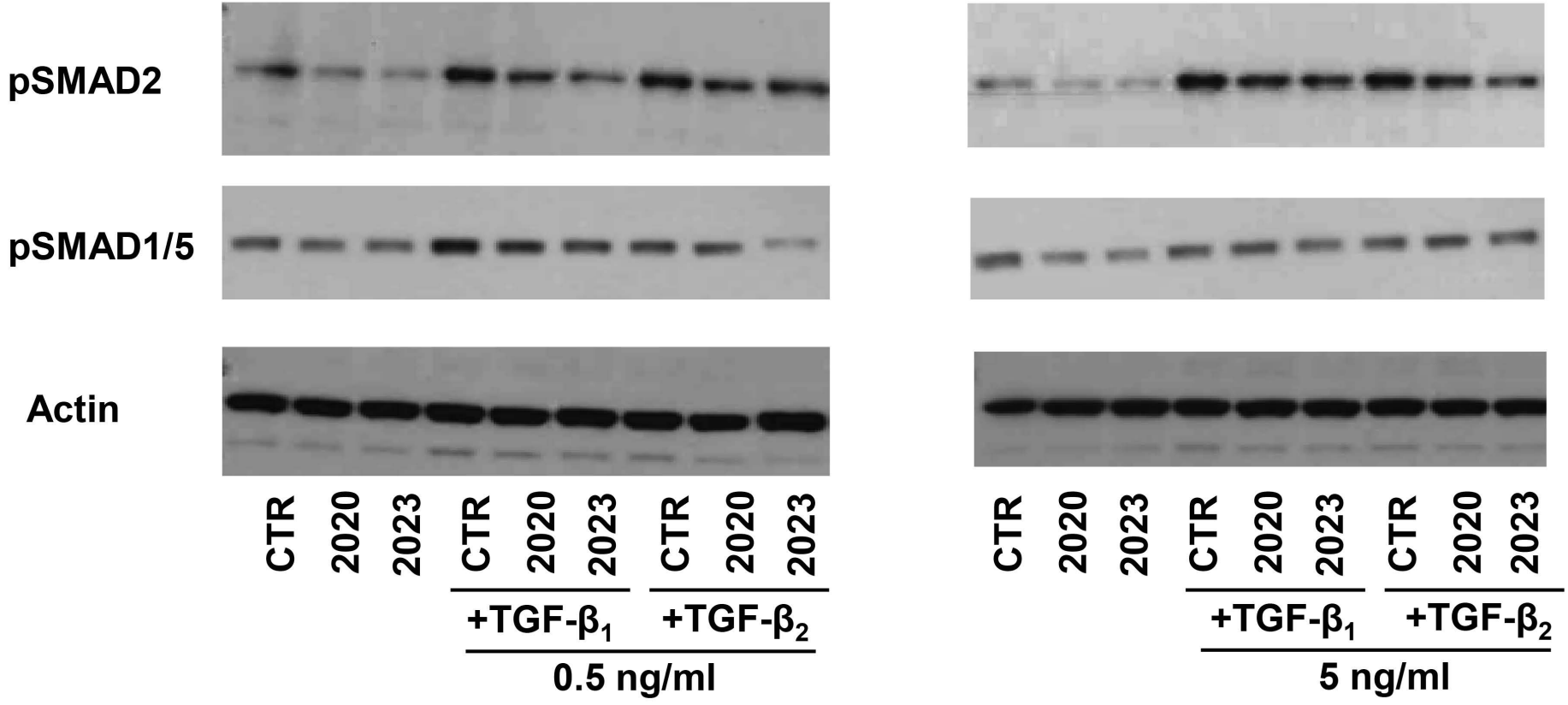
pSMAD2
pSMAD1/5
Actin
CTR
2020
2023
CTR
2020
2023
CTR
2020
2023
+TGF-β1
+TGF-β2
0.5 ng/ml
CTR
2020
2023
CTR
2020
2023
CTR
2020
2023
+TGF-β1
+TGF-β2
5 ng/ml

Figure 6

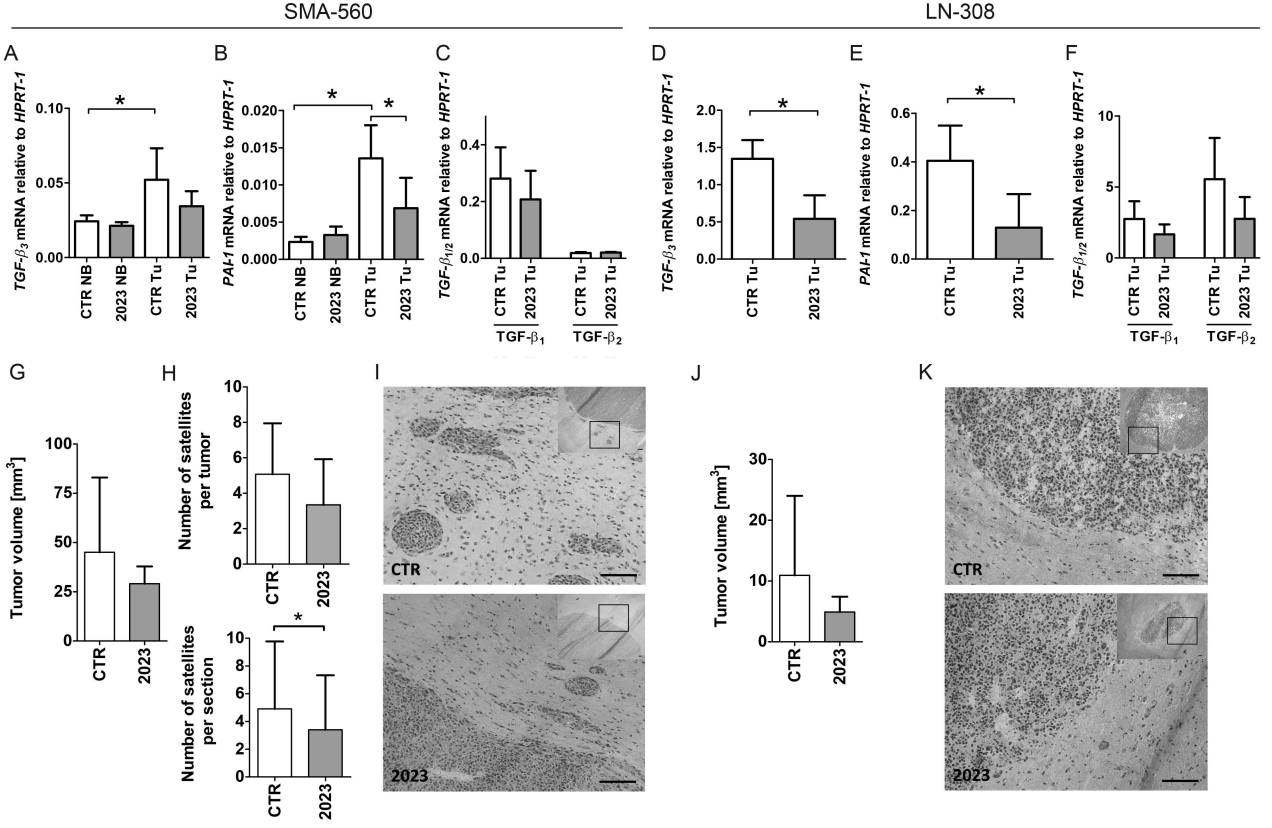
SMA-560
LN-308
A
B
C
D
E
F
TGF-β3 mRNA relative to HPRT-1
PAI-1 mRNA relative to HPRT-1
TGF-β1/2 mRNA relative to HPRT-1
CTR NB
2023 NB
CTR Tu
2023 Tu
TGF-β1
TGF-β2
G
H
I
J
K
Tumor volume [mm3]
Number of satellites per tumor
Number of satellites per section
CTR
2023

Supplementary Figure 1. Structure of ISTH2020 and ISTH2023

A-B. Schematic of the synthetic 15-mer antisense phosphorothioate oligonucleotides ISTH2020 (A) and ISTH2023 (B) sodium salt modified with locked nucleic acid (LNA) nucleosides ('3+3' LNA-modified gapmer)

Supplementary Figure 2. TGF-β_3 expression and patient survival, stratified for Verhaak subtypes – an analysis of the TCGA database.

Kaplan-Meier estimation for overall survival probability of patients with high (blue curve) versus low (red curve) TGF-β_3 mRNA expression derived of the TCGA database with data of > 500 glioblastoma patients stratified in the four different Verhaak subtypes, i.e. the neural, proneural, mesenchymal and classic subtype. The cut-off to segregate patients into groups of high and low expression was defined by the expression level that results in the highest association with survival (A) or by the median expression level of the target (B). Statistical significance (p) as assessed by log-rank test is indicated.

Supplementary Figure 3. Expression of TGF-$\beta_{1,2,3}$ in human and murine glioma cell lines.

Human glioma LTC and GIC (A) and murine LTC (means and SD) *in vitro* (B) and *ex vivo* (C) were analyzed for expression of *TGF-$\beta_{1,2,3}$* by RT-PCR. As a control for *ex vivo* samples, normal syngeneic mouse brain (NB) was included. Results are expressed as means of duplicates (A) or means and SD of for n=3 independent cell line samples and n=1 for NB (B, C). Statistical significance was assessed by one-way ANOVA and Bonferroni post-hoc testing (B, C).

Supplementary Figure 4: Validation of TGF-β antibodies.

Immunoblot loaded with human recombinant TGF-$\beta_{1,2,3}$ and analysed using antibodies to TGF-β_1 (G1221), TGF-β_2 (ab36495) or TGF-β_3 (ab15537).

Supplementary Figure 5: TGF-β_3-targeted oligonucleotides: effects on viability and proliferation. A. Viable or dead LN-308 cells were quantified by trypan blue-based automatic cell counting at 24, 48, 72 or 96 h after lipofection-aided transfection with oligonucleotides at 50 nM. Shown are means and SD of triplicates of a representative experiment. Viable or dead cells after transfection with control oligonucleotides were compared with the treatment with ISTH2020 and ISTH2023 oligonucleotides using one-way ANOVA and Bonferroni post-hoc testing showing no significant differences ($p>0.05$). B. LN-308 cells were treated with 2.5 µM of oligonucleotides for 4 to 8 days. Viable or dead cells were assessed as in A. Shown are means and SD of 4 replicates of a representative experiment.

Supplementary Figure 6. TGF-β_3 gene silencing does not affect TGF-β_1 and TGF-β_2 protein levels.

A-B. Cell culture supernatant of LN-308 cells was analysed for TGF-β_1 and TGF-β_2 after treatment with control or TGF-β_3-targeted oligonucleotide via lipofection (25 nM, 120 h after transfection, A) or gymnotic transfection (2.5 µM, day 8, B).

Supplementary Figure 1

A

ISTH2020: 5´*TTT*GTTTACACT*TCC*-3´

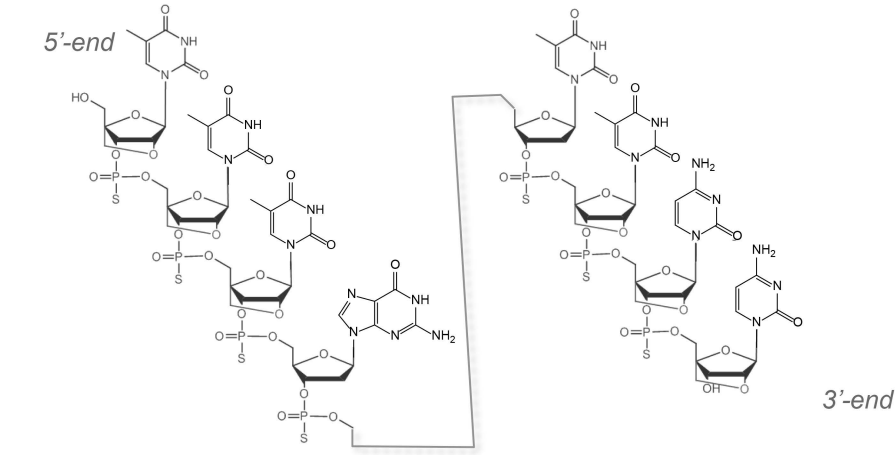

B

ISTH2023: 5´*GAG*TTTTTCCTT*AGG*-3´

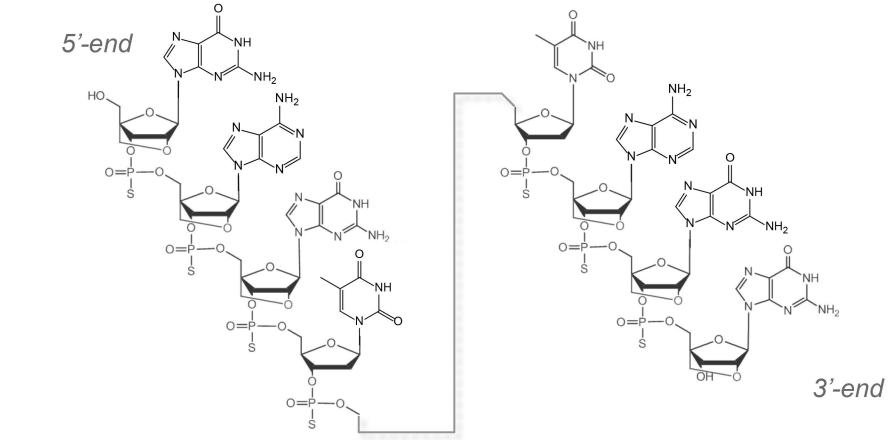

Supplementary Figure 2

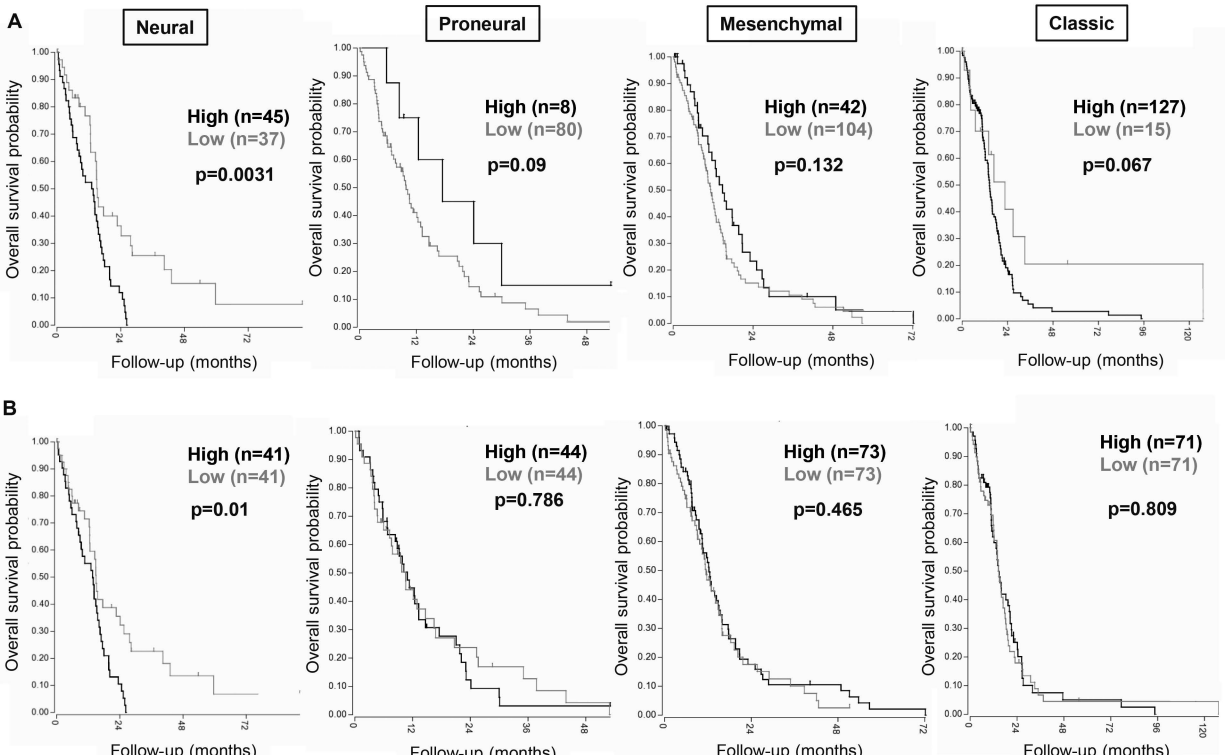

Supplementary Figure 3

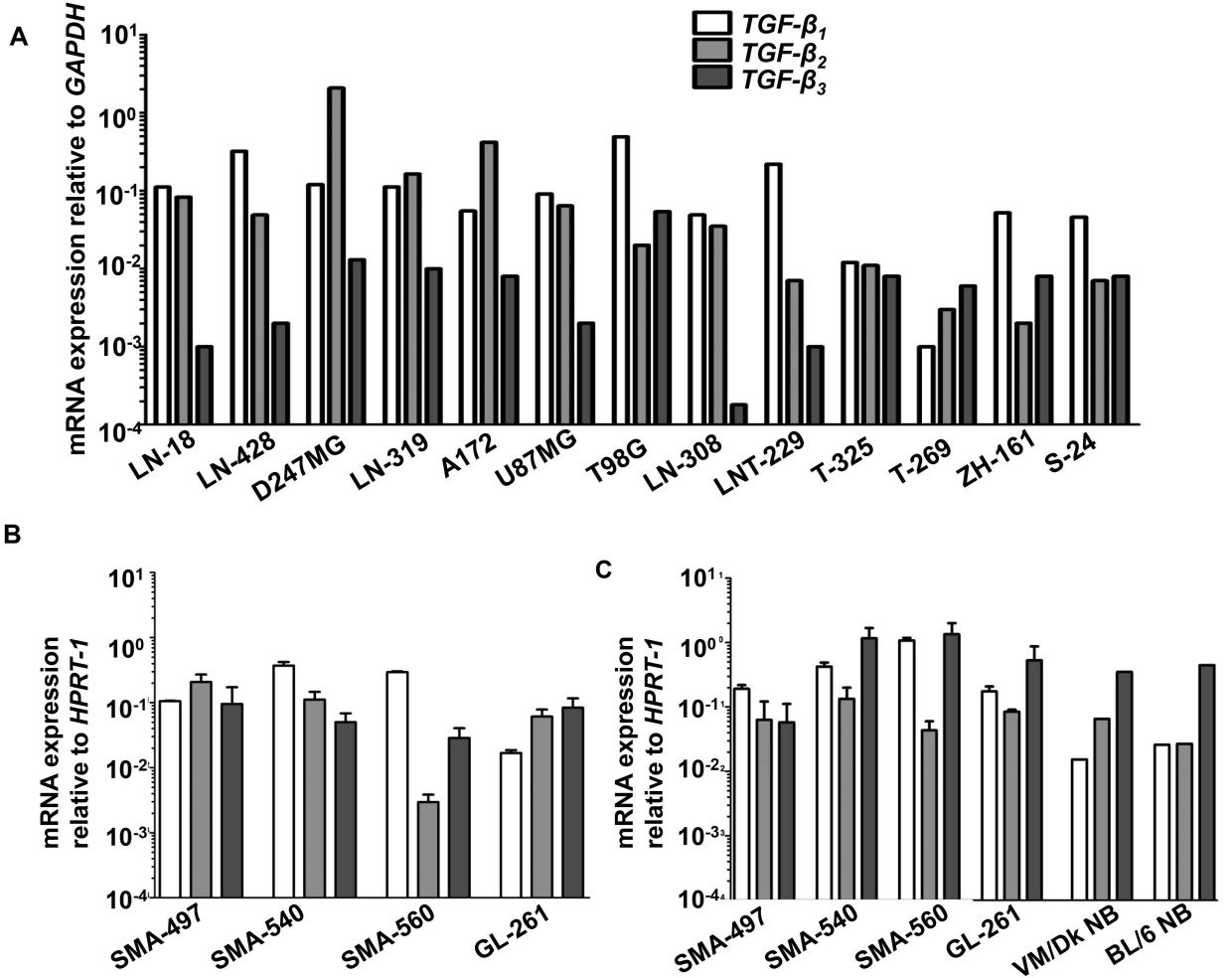

Supplementary Figure 4

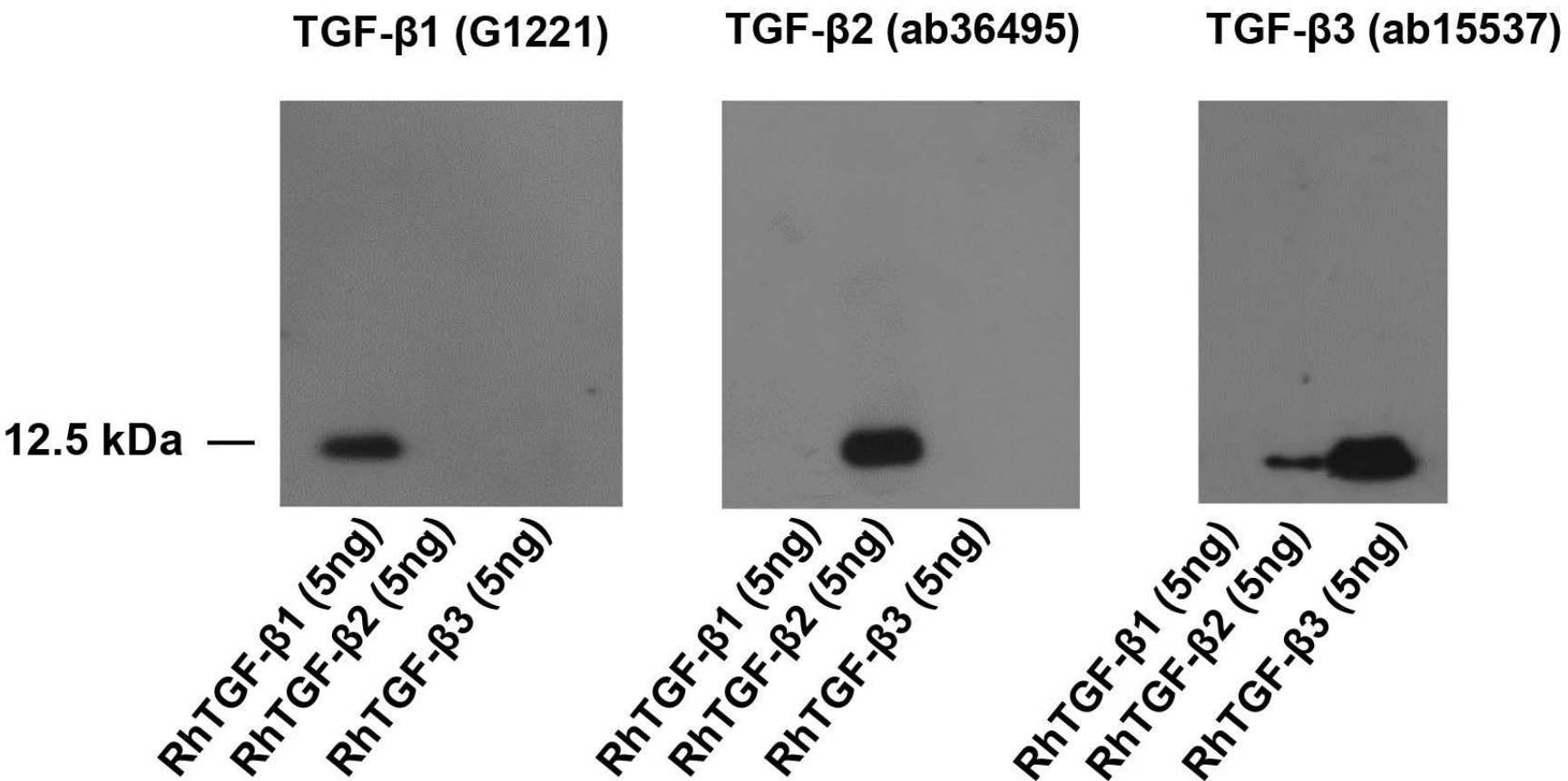

Supplementary Figure 5

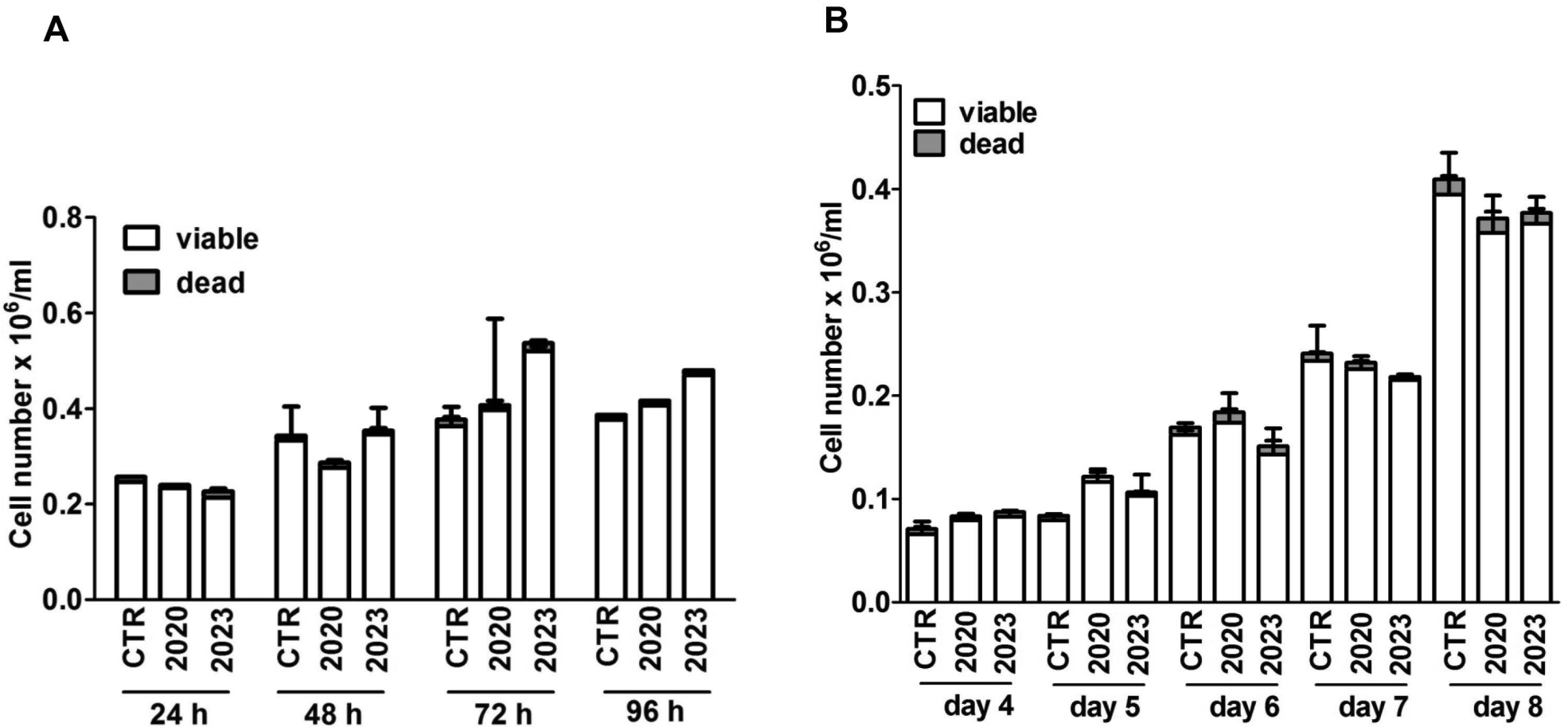

Supplementary Figure 6

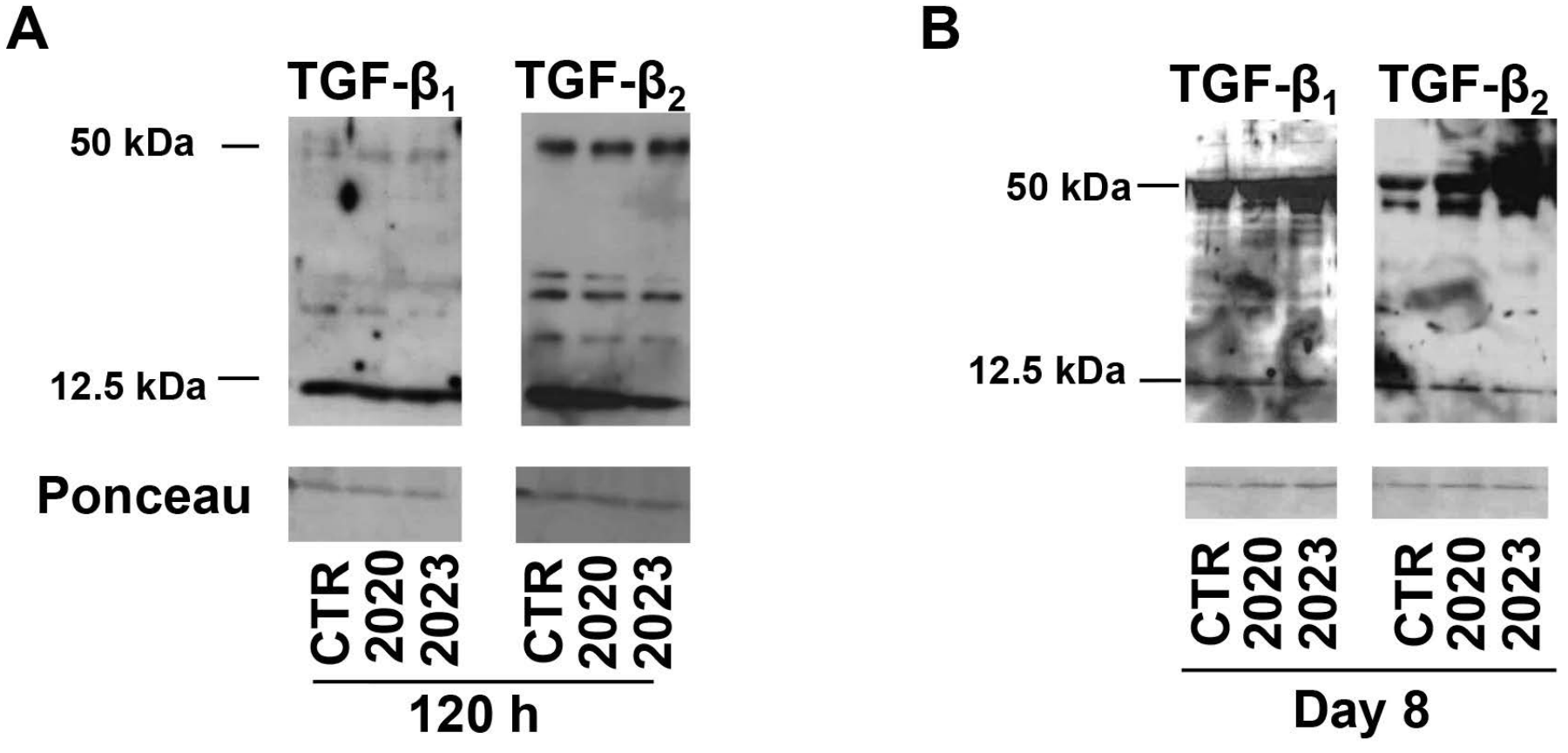

Supplementary material

Real time PCR

The following primer sequences were used: human *ARF-1* (forward 5'-TCC CAC ACA GTG AAG CTG ATG-3', reverse 5'-GAC CAC GAT CCT CTA CAA GC-3'), human *TGF-β1* (forward 5′-GCCCTGGACACCAACTATTG-3′, reverse 5′-CGTGTCCAGGCTCCAAATG-3′), human *TGF-β2*, (forward 5′-AAGCTTACACTGTCCCTGCTGC-3′, reverse 5′-TGTGGAGGTGCCATCAATACCT-3′), human *TGF-β3* (forward 5′-ATG ACC CAC GTC CCC TAT CA-3′, reverse 5′-CAG ACA GCC AGT TCG TTG TG-3′), murine *HPRT-1* (forward 5'-TTGCTGACCTGCTGGATTAC -3', reverse 5'-TTTATGTCCCCCGTTGACTG -3), murine *TGF-β1* (forward 5′- TGGAGCAACATGTGGAACTC -3′, reverse 5′-GTCAGCAGCCGGTTACCA -3′), murine *TGF-β2*, (forward 5′-GCCCACTTTCTACAGACCCT -3′, reverse 5′- CCTTGCTATCGATGTAGCGC -3′), murine human *TGF-β3* (forward 5′-AGCATCCACTGTCCATGTCA-3′, reverse 5′-TTCTTCCTCTGACTGCCCTG-3′), murine *ARF-1* (forward 5'-TCAGCTTCACCGTGTGGGATGT-3′, reverse 5′-CCTCGTTCACACGCTCTCTGTC). For expression analysis of human targets in oligonucleotide-treated xenograft mouse models, the following human-specific primers were used: *TGF-β1* (forward 5′-CAATTCCTGGCGATACCTCAG-3′, reverse-5′-GCACAACTCCGGTGACATCAA-3′), *TGF-β2* (forward 5′-CAGCACACTCGATATGGACCA-3′, reverse 5′-CCTCGGGCTCAGGATAGTCT-3′), *TGF-β3* (forward 5′-AACGGTGATGACCCACGTC-3′, reverse 5′-CCGACTCGGTGTTTTCCTGG-3′), *plasminogen activator inhibitor (PAI)-1* (forward 5′-CAGAAAGTGAAGATCGAGGTGAAC-3′, reverse 5′-GGAAGGGTCTGTCCATGATGAA-3′), *HPRT1* (forward 5′-TGAGGATTTGGAAAGGGTGT-3′, reverse 5′- GAGCACACAGAGGGCTACAA-3′).

Immunoblot (antibody information)

The following antibodies were used: anti-pSMAD2 (3108S), anti-pSMAD1/5 (41D10, both Cell Signaling, Boston, MA), anti-β-actin (sc-1616, Santa Cruz Biotechnology, Santa Cruz, CA), anti-GAPDH (EB07069, Everest Biotech, Oxfordshire, UK), anti-TGF-β_1 (G1221, Promega, Madison, MI), anti-TGF-β_2 (ab36495), anti-TGF-β_3 (ab15537).